Applied Catalysis B: Environmental 174–175 (2015) 113–119

Contents lists available at ScienceDirect

Applied Catalysis B: Environmental

journal homepage: www.elsevier.com/locate/apcatb

Photocatalytic ozonation of model aqueous solutions of oxalic and oxamic acids

C.A. Orge*, M.F.R. Pereira, J.L. Faria

LCM – Laboratório de Catálise e Materiais – Laboratório Associado LSRE–LCM, Departamento de Engenharia Química, Faculdade de Engenharia, Universidade do Porto, Rua Dr. Roberto Frias s/n, 4200-465 Porto, Portugal

ARTICLE INFO

Article history:
Received 19 December 2014
Received in revised form 22 February 2015
Accepted 27 February 2015
Available online 28 February 2015

Keywords:
Photocatalytic ozonation
Titanium dioxide
Carbon nanotubes
Oxalic acid
Oxamic acid

ABSTRACT

Degradation of aqueous solutions of oxalic acid (OXA) and oxamic acid (OMA), the final oxidation products of several organic compounds, has been investigated by photocatalytic ozonation. The combined method was carried out comparing P25 to synthesized sol–gel TiO_2, and composites of TiO_2 and multi-walled carbon nanotubes (MWCNTs) obtained either by the sol–gel method or by the hydration–dehydration technique. Photo-ozonation in the presence of P25 resulted in total conversion of OXA after 15 min. Concerning OMA, P25 and composites containing 80 and 90% wt of P25 led to complete degradation more rapidly. The reaction rate constants, k_{app}, were 15×10^{-2} min^{-1} for P25, 8.8×10^{-2} min^{-1} and 8.2×10^{-2} min^{-1} for the composite with 80 and 90% wt of P25, respectively. OMA removal by photocatalytic ozonation is here reported for the first time and a remarkable conversion is obtained with complete degradation achieved in a short period of time in the presence of TiO_2, P25 and composites with 80 and 90%wt of P25 and MWCNTs and with 80%wt of P25 and oxidized MWCNTs. By performing single photocatalysis or single ozonation for selected materials, a synergetic effect of the combined method was identified.

1. Introduction

Advanced oxidation processes (AOPs) are efficient in accelerate the non-selective oxidation of organics and thus the mineralization of a wide range of recalcitrant compounds resistant to conventional treatments [1–3]. AOPs are based on the generation of highly reactive free radicals by using chemical and/or other forms of energy, and under appropriate conditions the species to be removed are totally converted to CO_2, H_2O and inoffensive mineral salts. Photocatalysis ranks among the AOPs that proved advantageous in remediation of contaminate waste water, although large-scale application remains somewhat expensive owing to the cost of artificial photons and slow oxidation kinetics. The fundamental mechanism of photocatalysis consists in the irradiation of a semiconductor material by light with sufficient energy to excite the electrons from the valence to the conduction band generating electron–hole pairs, which migrate to the surface where they can react with adsorbed OH^- to produce $HO^\bullet$; or directly oxidize other adsorbed species [4]. In this process, oxygen is widely used as compensatory oxidant to complete the electron balance. The disadvantage is that mineralization normally requires long reaction time due to the slow electron transfer [5]. In order to improve the performance of photocatalytic processes, different strategies have been followed, such as adding oxidant species as hydrogen peroxide, Fe^{2+} ions or ozone (O_3).

The use of O_3 for the destruction of organic compounds is a recognized water treatment technique. O_3 is a strong oxidative agent ($E^\circ = 2.07$ eV) and reacts directly via molecular O_3, and indirectly by the hydroxyl radicals ($HO^\bullet$), which are a powerful and non-selective oxidant ($E^\circ = 2.8$ eV) [6].

Photocatalytic ozonation is an emergent technology that combines two AOPs with the main advantage of this integrate process being the highest $HO^\bullet$ yield due to the more powerful oxidant character of ozone compared to oxygen [7]. Thus, an additional and important way of $HO^\bullet$ formation is the O_3 capture of electrons in the conducting band of the catalyst to yield the ozonide ion radical ($O_3^{\bullet -}$) that eventually gives rise to $HO^\bullet$ [8]. This advantage, on the other hand, minimizes the undesirable recombination reaction of electrons and positive holes in the valence band, which results in the inhibition of the process rate.

Most of the publications on photocatalytic ozonation applied suspensions of fine TiO_2 particles, often in the form of P25 (Evonik; Degussa), the most used photocatalyst, characterized by its non-toxicity, photo-stability, as well as by its low cost and very high efficiency under ultraviolet irradiation. Electron–hole recombination limits the efficiency of TiO_2 photocatalysis. As a strategy to prevent this, TiO_2/carbon materials in simple mixtures or as

* Corresponding author. Tel.: +351 225081400; fax: +351 225081440.
E-mail addresses: carlaorge@fe.up.pt (C.A. Orge), fpereira@fe.up.pt (M.F.R. Pereira), jlfaria@fe.up.pt (J.L. Faria).

http://dx.doi.org/10.1016/j.apcatb.2015.02.038
0926-3373/

nanocomposites have been investigated. Mixed- phase TiO_2-based composites tend to show higher photoreactivity in comparison to pure-phase materials, as exhibited by P25, due to the formation of solid–solid interfaces that facilitate charge transfer and spatial separation, reducing electron–hole recombination, and interfacial defect sites that act as "hot spots" [9] .

The aim of the present work relies on the investigation of oxalic acid (OXA) and oxamic acid (OMA) degradation by photocatalytic ozonation. For this study, composites with titanium dioxide (TiO_2) and multi-walled carbon nanotubes (MWCNTs) were prepared by different procedures and with diverse compositions. Experiments only with catalytic ozonation or photocatalysis using the prepared materials were also carried out in order to better understand the results.

Many effluents, especially in metallurgical and textile industrial waste waters contain OXA. Furthermore, OXA is a detectable intermediate in the mineralisation of many pesticides and other organic compounds [10].

On the other hand, OMA is normally generated from the oxidation of organic compounds containing nitrogen functional groups, as aniline, sulfanilic acid and azo dyes [11,12]. OMA is highly refractory to chemical oxidation and conventional processes as ozonation and photolysis did not allow its mineralization. Very few information on this compound was found in the literature and the development of an efficient process capable of removing this compound is an important step to mineralize a vast range of organic pollutants. To the best our knowledge, no papers in the literature described OMA removal by photocatalytic ozonation. OMA removal by catalytic ozonation in the presence of activated carbon, carbon nanotubes and ceria- activated carbon composites was previously studied [13–16]. The best results allowed 70% and 75% removal after 10 h of reaction in the presence of MWCNTs with basic properties and ceria-activated carbon composite with 10% of cerium oxide, respectively. However, total removal was never achieved even for long reaction times. OMA degradation was also studied by an electrochemical AOP. Total degradation was achieved at 270 min of reaction by anodic oxidation with a boron-doped diamond electrode and Fe^{2+} solution under UVA illumination [17]. In another work, OMA was transformed to carbonates and nitrogen with 88.2% conversion, in NaOH medium, with Pd/CNT modified electrode [18].

2. Experimental

2.1. Reagents and materials

Titanium (IV) isopropoxide ($Ti[OCH(CH_3)_2]_4$, 97%), nitric acid (HNO_3, ≥65%), oxalic acid ($C_2H_2O_4$, ≥99%) and oxamic acid ($C_2H_3O_3N$, ≥98%) were purchased from Sigma–Aldrich. Ethanol (C_2H_5OH, 99.5%) was obtained from Panreac. Sulfuric acid was supplied by Fisher Scientific. Commercial TiO_2, sample P25, was supplied by Evonik Degussa Corporation. The commercial multi-walled carbon nanotubes, MWCNTs, were supplied by Nanocyl (ref. 3100). Ultrapure water was produced on a Direct-Q milipore system.

2.2. Catalyst preparation and characterization

Different sets of catalysts were prepared. The composites with TiO_2 and MWCNTs were synthesized by the sol–gel method to match 20, 50 and 80 wt.% of TiO_2 (after designated 20%TiO_2/MWCNTs, 50%TiO_2/MWCNTs and 80%TiO_2/MWCNTs, respectively). Neat sol–gel TiO_2 was also prepared (hereafter referred as TiO_2).

The composites of P25 and MWCNTs were prepared using the hydration–dehydration technique in the same ratios used for sol–gel (samples 20%P25/MWCNTs, 50% P25/MWCNTs and 80% P25/MWCNTs) and two additional composites with 90 and 95% of P25 (samples 90% P25/MWCNTs and 95% P25/MWCNTs, respectively).

The TiO_2 sample was prepared by the slowly addition of $Ti[OCH(CH_3)_2]_4$ to ethanol. After 30 min under continuous stirring, nitric acid was added. The solution was loosely covered and kept stirring until the homogenous gel formed. After grinding the xerogel, a fine powder was formed and afterwards it was calcined at 400 °C in a nitrogen flow for 2 h [19] .

TiO_2/MWCNTs composites were prepared by a similar procedure to that described to TiO_2 sample, where a given amount of MWCNTs was dispersed in the metal solution 2 h after adding nitric acid.

In the preparation of P25/MWCNTs composites, a selected amount of MWCNTs was dispersed in water under ultrasonication. P25 was added to the suspension 30 min later and the mixture was heated up to 80 °C and magnetically stirred until the water was completely evaporated. The resulting composite was dried at 110 °C overnight.

The textural characterization of the materials was based on the corresponding N_2 equilibrium adsorption/desorption isotherms, determined at −196 °C with a Quantachrome Instruments NOVA 4200e apparatus. The relative amount of TiO_2 in the catalyst was determined by thermogravimetric analysis (TG) under air in a STA 409 PC/4/H Luxx Netzsch thermal analyser.

2.3. Catalytic experiments

Experiments of photocatalytic ozonation (O_3 + UV/catalyst), catalytic ozonation (O_3/catalyst) and photocatalysis (UV/catalyst) were performed on OXA and OMA. Photo-ozonation (O_3 + UV), single ozonation (O_3) and photolysis (UV) were also carried on as control. A glass immersion photochemical reactor (diameter: 60 mm; height: 250 mm) loaded with 250 cm^3 of solution. The reactor was equipped with a Heraeus TQ 150 medium-pressure mercury vapor lamp located axially and a DURAN 50® glass cooling jacket was placed around the lamp (main resulting emission lines at λ_{exc} = 365, 405, 436, 546 and 578 nm). The initial concentration of OXA and OMA was of 1 mM. The agitation was maintained constant at 400 rpm in order to keep the reactor content perfectly mixed. The gas was bubbled in the reactor by a diffuser with 1 cm of diameter. The experiments were performed at constant gas flow rate (150 cm^3 min^{-1}) and constant inlet ozone concentration (50 g m^{-3}). In O_3 containing experiments, ozone was produced from pure oxygen in a BMT 802X ozone generator. The concentration of ozone in the gas phase was monitored with a BMT 964 ozone analyser. Ozone in the gas phase leaving the reactor was removed in a series of gas washing bottles filled with potassium iodide solution. In direct photolysis and photocatalytic reactions, the ozone-containing stream was replaced by an oxygen stream.

The concentration of selected acids was determined by HPLC with Hitachi Elite Lachrom system equipped with an ultraviolet detector. The stationary phase was an Altech AO-100 column working at room temperature under isocratic elution with H_2SO_4 5 mM at a flow rate of 0.5 cm^3 min^{-1}. The injection volume was 15 μL and the detector wavelength was 200 nm.

3. Results and discussion

3.1. Characterization of the catalysts

The TiO_2 average content (determined by thermal analyses) and the BET surface area (from the N_2 adsorption–desorption isotherms) of the prepared composites is collected in Table 1.

Table 1
BET surface area of prepared samples.

Sample	%TiO_2[a]	S_{BET}($m^2\,g^{-1}$)
MWCNTs	–	280
TiO_2	–	80
20%TiO_2/MWCNTs	24	230
50%TiO_2/MWCNTs	48	200
80%TiO_2/MWCNTs	79	150
P25	–	50
20%P25/MWCNTs	20	260
50%P25/MWCNTs	50	180
80%P25/MWCNTs	78	100
90%P25/MWCNTs	86	70
95%P25/MWCNTs	90	60

[a] TiO_2 average content determined by TG.

Prepared TiO_2 has a higher BET surface area than commercial P25. As expected, the BET surface area increases with the amount of MWCNTs presented in the composites, independently of the preparation method, due to the contribution of carbon material. No significant differences were observed between the expected and the determined (by TG analysis) masses of TiO_2, indicating that the materials were successfully prepared.

The N_2 isotherms of MWCNTs, bare TiO_2 and some prepared composites are depicted in Fig. 1.

The isotherm of synthetized TiO_2 is of type IV with a hysteresis loop that can be ascribed to type H2 accordingly to IUPAC classification, while the isotherms of P25 and MWCNTs can be classified as type II [20].

3.2. Removal of oxalic and oxamic acids

Carboxylic acids are important materials used by the chemical industry, such as in textile, paper, detergents, plastics and pharmaceutical, and they are often obtained as aqueous solutions. In fact, OXA has been identified as one of the most important final products of non-catalytic oxidation processes. In addition to be a common final oxidation product presents a simple molecular structure and is directly oxidized to CO_2 without the formation of any intermediates allowing better interpretation of the results. In this context, OXA was selected for preliminary studies. Photocatalytic ozonation of OXA was carried out in the presence of P25. Photocatalysis (UV/P25) and catalytic ozonation (O_3/P25), as well as the respective reactions without catalyst were also performed. All experiments were carried out at the natural pH of the solution (2.9 ± 0.1). The conversion curves are presented in Fig. 2.

A first order kinetic model was considered to fit the experimental data. In the absence of any solid catalyst, the evolution of OXA

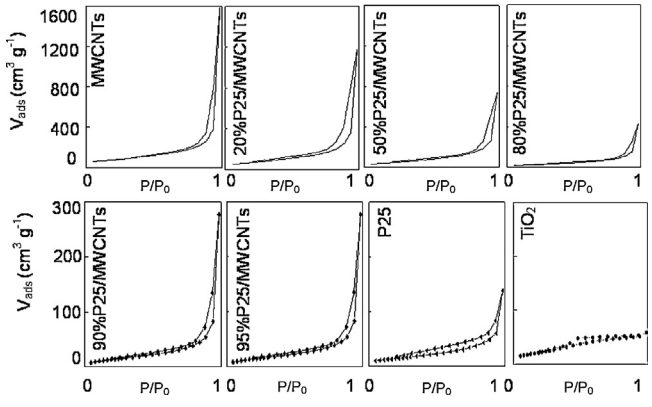

Fig. 1. N_2 adsorption–desorption isotherms for MWCNTs, bare TiO_2 samples and composites of P25 and MWCNTs.

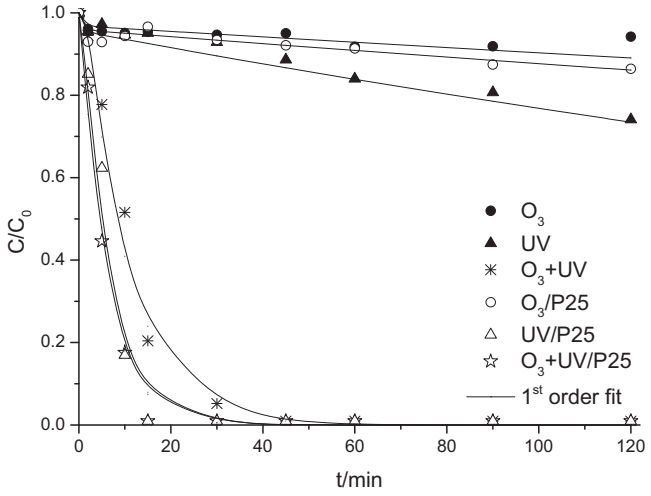

Fig. 2. OXA removal using P25 as catalyst.

Table 2
First-order rate constants (homogeneous or apparent) for oxidation of OXA.

System	$k/10^{-2}\,min^{-1}$
O_3	0.07 ± 0.02[a]
UV	0.22 ± 0.02[a]
O_3 + UV	10.7 ± 0.4[a]
O_3/P25	0.09 ± 0.02[b]
UV/P25	18 ± 3[b]
O_3 + UV/P25	18 ± 1[b]

[a] k_{hom}.
[b] k_{app}.

concentration during the oxidation process was found to be well described by the following equation:

$$-\frac{dC_{pollutant}}{dt} = k_{hom}C_{pollutant} \quad (1)$$

where k_{hom} (min^{-1}) represents the first-order apparent rate constant and $C_{pollutant}$ (mM) is the concentration of the selected pollutant in each instant. Integration of Eq. (1), considering $C_{pollutant} = C_{pollutant,0}$, when $t = 0$, leads to:

$$\ln\frac{C_{pollutant,0}}{C_{pollutant}} = k_{hom}t \quad (2)$$

When the prepared materials are introduced, both homogeneous and heterogeneous degradation occur. Therefore, the pollutant removal rate is the sum of the two contributions:

$$-\frac{dC_{pollutant}}{dt} = (k_{hom} + k_{het})C_{pollutant} \quad (3)$$

where k_{het} (min^{-1}) represents the first-order apparent rate constant for the heterogeneous degradation. Integration of Eq. (3), considering $k_{app} = k_{hom} + k_{het}$ and $C_{pollutant} = C_{pollutant,0}$, when $t = 0$, leads to:

$$\ln\frac{C_{pollutant,0}}{C_{polllutant}} = k_{app}t \quad (4)$$

Apparent first-order rate constant values of OXA degradation are listed in Table 2.

As previously reported, OXA is refractory to single ozonation [13]. Ozonation catalyzed by P25 removed less than 20% after 2 h of reaction. As stated before, photolysis only removed 26% after 2 h of reaction. But when UV radiation is combined with ozone all OXA is removed after 45 min of reaction. The introduction of the selected catalyst in UV irradiation system increased the mineralization rate 82 times when compared with neat photolysis ($0.22 \times 10^{-2}\,min^{-1}$).

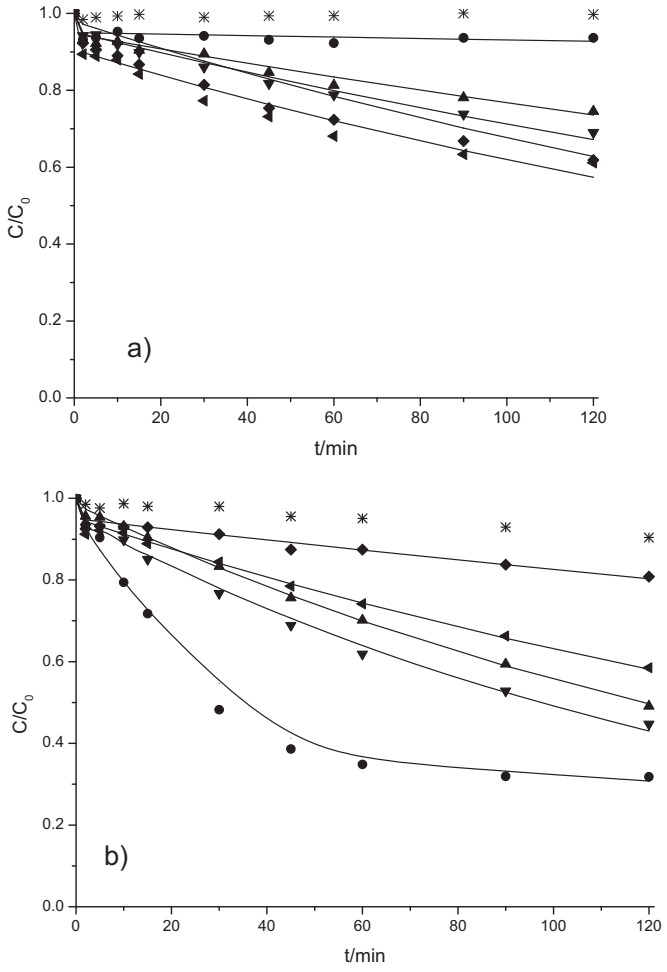

Fig. 3. OMA degradation by catalytic ozonation (a) and photocatalysis (b) in the presence of TiO_2/MWCNTs composites: (*) non-catalytic run; (●) TiO_2; (▲) MWCNTs; (♦) 20%TiO_2/MWCNTs; (◄) 50%TiO_2/MWCNTs; (▼) 80%TiO_2/MWCNTs; (—) 1st order fit.

Under the experimental conditions, almost no differences were observed when ozone was introduced in the photocatalytic process carried out with P25. Although total removal was achieved when ozone and radiation were carried out together, when P25 was added the complete degradation is faster. Since OXA was easily removed by photo-ozonation, OMA, which is more refractory to oxidation than OXA, was selected for a more detailed study.

Photocatalytic ozonation of OMA was carried out with TiO_2/MWCNTs composites with different compositions and synthesized by different procedures. In order to better understand the results, photocatalysis and catalytic ozonation experiments were also carried out, including reactions with reference MWCNTs and TiO_2. All experiments were carried out at the natural pH of the solution (2.8 ± 0.1). Figs. 3 and 4 depict the results of OMA degradation by the individual methods and combined process, respectively.

The combination of the prepared composites with O_3 or UV light presented better performance than the correspondent reactions without catalysts. In the case of catalytic ozonation, all TiO_2/MWCNTs composites allowed better catalytic activities than TiO_2 or MWCNTs; however, the highest mineralization achieved was of 40% after 2 h of reaction. In photocatalysis, all composites had better performance than MWCNTs and the catalytic activity increases with the amount of TiO_2 presented in the composites. TiO_2 presented a better catalytic activity than composites, but total mineralization was not attained.

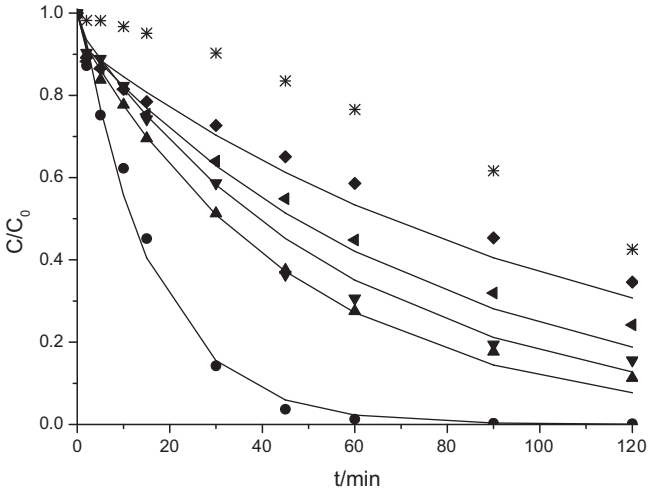

Fig. 4. OMA degradation by photocatalyticozonation in the presence of TiO_2/MWCNTs composites: (*) non-catalytic run; (●) TiO_2; (▲) MWCNTs; (♦) 20%TiO_2/MWCNTs; (◄) 50%TiO_2/MWCNTs; (▼) 80%TiO_2/MWCNTs; (—) 1st order fit.

Fig. 4 shows that similarly to what happened with individual methods, the addition of any of the prepared materials in the O_3 and UV light system resulted in better performance than that obtained by the non-catalytic combined method. TiO_2/MWCNTs composites presented worse performances than TiO_2 or MWCNTs. TiO_2 degraded all OMA presented in solution after 1 h of reaction and MWCNTs removed 89% after 2 h of reaction.

A similar study was carried out with P25/MWCNTs composites. Fig. 5(a) and (b) and Fig. 6 depict the results of catalytic ozonation, photocatalysis, and photocatalytic ozonation, respectively. Catalytic ozonation in the presence of P25/MWCNTs composites was not a good option to degrade OMA, since the best removal achieved was 15%, which is lower than the value obtained by MWCNTs. Comparing with catalytic ozonation, photocatalysis carried out with P25/MWCTs composites seems to be a better alternative, leading to higher conversions. All composites performed better than MWCNTs and the composites with 80, 90, and 95% P25 removed more than 70% of OMA after 2 h of reaction. However, these composites had a worse catalytic activity than P25, which removed 84% after 2 h of reaction. Marques et al. reported similar results during photocatalysis of caffeine solutions in the presence of composites with functionalized MWCNTs and P25 [21]. When MWCNTs are combined with P25, a significant decrease of the photocatalytic activity was always observed, regardless the content of carbon nanotubes. On the other hand, Sampaio et al. stated that there is an optimal carbon nanotube loading in the degradation of methylene blue by photocatalysis [22]. In the case of photocatalytic ozonation, P25 presented the best catalytic activity, allowing total degradation after 30 min of reaction. However, with the exception of samples with 20% and 50% of P25, the remaining composites also achieved total OMA degradation in 45 or 60 min of reaction, showing to be effective catalysts. Similar to what happened with composites prepared by the sol–gel procedure, photocatalytic ozonation presented the best results compared to catalytic ozonation and photocatalysis.

Apparent first-order rate constant values for photocatalytic ozonation systems are listed in Table 3. For the fitting procedure, the value of k_{hom} previously calculated was fixed. Under the conditions used, P25, which consists of both anatase and rutile crystalline phases, is the most effective catalyst for OMA degradation. When carbon nanotubes were combined with P25 a decrease was always observed, with the pseudo first-order rate constant decreasing from 15×10^{-2} min^{-1} for bare P25 to under 8×10^{-2} min^{-1} for the composites with 80 and 90% of P25. For composites prepared by the

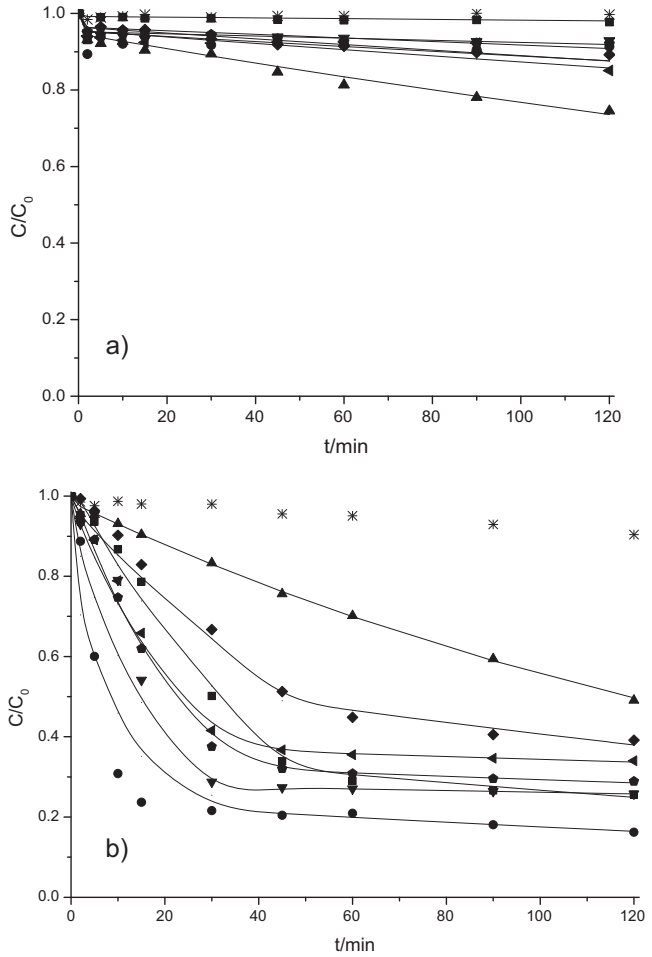

Fig. 5. OMA degradation by catalytic ozonation (a) and photocatalysis(b) in the presence of P25/MWCNTs composites: (*) non-catalytic run; (●) P25; (▲) MWCNTs; () 20%P25/MWCNTs; (◄) 50%P25/MWCNTs; (▼) 80%P25/MWCNTs; (⬟) 90%P25/MWCNTs; (■) 95%P25/MWCNTs; (—) 1st order fit.

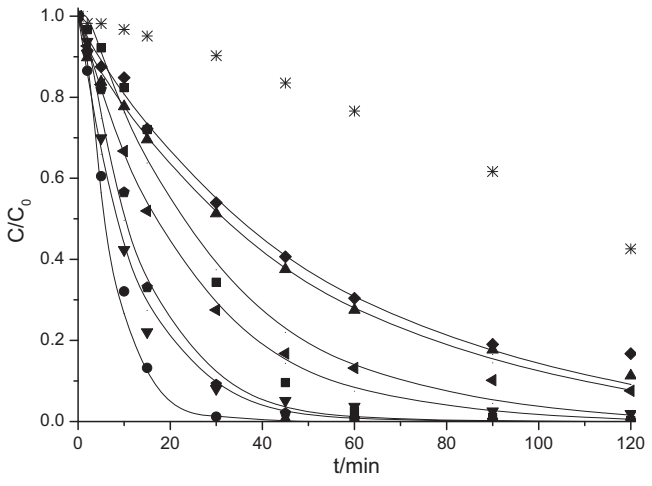

Fig. 6. OMA degradation by photocatalyticozonation in the presence of P25/MWCNTs composites: (*) non-catalytic run; (●) P25; (▲) MWCNTs; (⧫) 20%P25/MWCNTs; (◄) 50%P25/MWCNTs; (▼) 80%P25/MWCNTs; (⬟) 90%P25/MWCNTs; (■) 95%P25/MWCNTs; (—) 1st order fit.

Table 3
Apparent first-order rate constants for photocatalytic ozonation of OMA (determined from the initial 30 min of reaction).

System	k_{app} /10^{-2} min^{-1}
O_3 + UV	0.32 ± 0.02[a]
O_3 + UV/MWCNTs	2.1 ± 0.1
O_3 + UV/TiO_2	6.4 ± 0.4
O_3 + UV/20%TiO_2/MWCNTs	0.9 ± 0.2
O_3 + UV/50%TiO_2/MWCNTs	1.3 ± 0.2
O_3 + UV/80%TiO_2/MWCNTs	1.7 ± 0.1
O_3 + UV/P25	15 ± 1
O_3 + UV/20%P25/MWCNTs	2.0 ± 0.1
O_3 + UV/50%P25/MWCNTs	4.4 ± 0.1
O_3 + UV/80%P25/MWCNTs	8.8 ± 0.5
O_3 + UV/90%P25/MWCNTs	8.2 ± 0.4
O_3 + UV/95%P25/MWCNTs	3.6 ± 0.4

[a] k_{hom}.

sol–gel method, a pronounced decrease was also observed. The maximum pseudo first-order constant for TiO_2/MWCNTs composites was 1.7×10^{-2} min^{-1}, while for TiO_2 was 6.4×10^{-2} min^{-1}. Independently of the preparation method, when carbon nanotubes were combined with titanium dioxide, a decrease of the catalytic activity was observed when compared with the parent TiO_2. Analysing bare TiO_2 samples, the pseudo first-order rate constant obtained for P25 is approximately twice than that obtained for TiO_2. With the exception of 50%TiO_2/MWCNTs and 80%TiO_2/MWCNTs composites, the degradation rate of OMA by the combined method was found to be higher than the sum of the degradation rate of the individual treatments, which indicates the presence of a synergetic effect.

Photocatalytic ozonation in the presence of TiO_2 either prepared by the sol–gel procedure or commercial, and in the presence of composites containing high amount of P25 is an interesting alternative to remove OMA, a strongly refractory compound.

According to the literature, besides the direct ozonation, in the presence of TiO_2 under illumination, ozone can generate HO• radicals through the formation of an ozonide radical ($O_3^{\bullet -}$) in the adsorption layer [8]:

$$TiO_2 + h\nu \rightarrow TiO_2 + h^+ + e^- \quad (5)$$

$$O_3 + e^- \rightarrow O_3^{\bullet -} \quad (6)$$

$$h^+ + H_2O \rightarrow HO^\bullet + H^+ \quad (7)$$

The generated $O_3^{\bullet -}$ species rapidly reacts with H^+ in the solution to give $HO_3^\bullet$ radical, which evolves to give O_2 and HO• as shown below:

$$O_3^{\bullet -} + H^+ \rightleftarrows HO_3^\bullet \quad (8)$$

$$HO_3^\bullet \rightarrow HO^\bullet + O_2 \quad (9)$$

In absence of O_3, dissolved O_2 itself can accept TiO_2 conduction band electron and generate $O_2^{\bullet -}$

$$O_2^{\bullet -} + H^+ \rightleftarrows HO_2^\bullet \quad (10)$$

$$2HO_2^\bullet \rightarrow H_2O_2 + O_2 \quad (11)$$

$$H_2O_2 + O_2^{\bullet -} \rightarrow HO^\bullet + OH^- + O_2 \quad (12)$$

In contrast with $HO_3^\bullet$, this species cannot give HO• radicals in a single step. This mechanism requires a total of three steps for the generation of a single HO• species, which is a less favored situation if compared with the one electron needed through the $O_3^{\bullet -}$ reaction pathway.

Kopf et al. proposed a further possible reaction path [23]. In addition to direct ozone attack and direct electron transfer from TiO_2

to the ozone molecule, they suggested that oxygen should have an influence on the photocatalytic ozonation:

$$TiO_2 + h\nu \rightarrow TiO_2 + h^+ + e^- \quad (5)$$

$$e^- + O_2 \Leftrightarrow O_2^{\bullet -} \quad (13)$$

$$O_3 + O_2^{\bullet -} \rightarrow O_3^{\bullet -} + O_2 \quad (14)$$

$$O_3^{\bullet -} + H^+ \rightleftarrows HO_3^{\bullet} \quad (8)$$

$$HO_3^{\bullet} \rightarrow HO^{\bullet} + O_2 \quad (9)$$

The recombination of electrons and positive holes could be interfered by the reaction between ozone and electrons on the surface of titanium dioxide, Eq. (6). Consequently, a larger number of radicals is produced, thereby accelerating the photocatalytic reaction. The larger number of HO radicals produced when ozone, UV radiation and an appropriated catalyst are together justifies the high activity verified. The inclusion of a carbon phase decreased the performance of the semiconductor. Both composites prepared by sol–gel procedure or by the hydration–dehydration method did not match the performance of the reference TiO_2; nevertheless, composites containing 90% of P25 also showed good catalytic activity. According to the literature, composites prepared by the sol–gel method have limited homogeneity, since they usually form big semiconductor aggregates with very weak interaction with the carbon phase, while P25 containing composites showed a good distribution of TiO_2 along the walls of carbon nanotubes [21]. Replicated experiments of OMA removal in the presence of P25 and 90%P25/MWCNTs were carried out in order to evaluate the reproducibility of the results, since this is an important factor, especially for industrial applications. The results revealed maximum relative differences of 4% around the average conversion at 10 min and 30 min for P25 and 90%P25/MWCNTs, respectively (data not shown).

In order to verify the effect of the surface chemistry of MWCNTs in photocatalytic ozonation, an oxidation treatment with HNO_3 was carried out. After the functionalization, composites of treated MWCNTs with 80% of P25 and with 80% of TiO_2 were prepared by the hydration–dehydration technique (sample 80%P25/MWCNTs) and by the sol–gel method (sample 80%TiO2/MWCNTs) as previous described.

The evolution of oxamic acid during photocatalytic ozonation in the presence of composites with oxidized MWCNTs is depicted in Fig. 7.

The introduction of oxidized MWCNTs in the composites decreases the catalytic activity, especially in the case of the composite prepared by the sol–gel method. Although the performance of the composite with 80%P25/MWCNTs_oxi (functionalized MWCNTs) prepared by the hydration–dehydration was inferior to the corresponding composite with original MWCNTs, OMA was completely removed by photocatalytic ozonation. This result is at variance with the reported in caffeine degradation by photocatalysis with TiO_2 and MWCNTs composite [21]. In that work, the oxygenated groups introduced on MWCNTs play an important role in the catalytic activity, increasing from 37% to 88% of caffeine conversion. The reason there given was that the nitric acid treatment introduced a large amount of oxygenated groups on the surface of carbon nanotubes, which promotes the dispersion of TiO_2 particles in the composites and formation of Ti—O—C bonds, as in esterification reactions between the carboxylic acid groups of carbon nanotubes and the hydroxyl groups of TiO_2. However the situation is not directly comparable with the present one, since ozonation processes are favored by carbon nanotubes with low acidic character [16,24]. The ozone decomposition into radicals on the surface of carbon materials is preceded by an adsorption step where ozone is adsorbed on the carbon surface. The ozone molecules have a higher affinity for basic carbons, which are known to have a high density of delocalized π electrons on the basal planes. Consequently, carbon materials with less acidic character have a higher catalytic activity for ozone decomposition. The experimental results suggest that the negative effect caused by the presence of acid groups on the MWCNTs surface overlays the positive effect, since photocatalytic ozonation with oxidized MWCNTs was less efficient than with original MWCNTs, as happens in the catalytic ozonation.

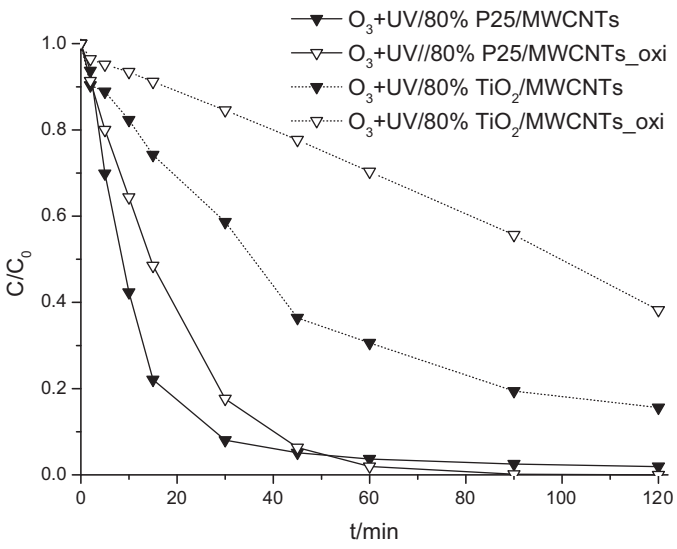

Fig. 7. OMA degradation during photocatalytic ozonation in the presence of composites with original and oxidized MWCNTs.

4. Conclusions

The mineralization of two carboxylic acids, OXA and OMA, known as final oxidation products of a large number of organic compounds, was carried out by photocatalytic ozonation. For that purpose, composites of TiO_2 and MWCNTs with several compositions, prepared by different methods, as well as reference TiO_2 prepared by the sol–gel procedure or commercially obtained P25 were tested as catalysts.

Photocatalytic ozonation was proven to be an efficient process for the removal of carboxylic acids from aqueous solution. In the case of OXA, P25 achieved total degradation after 15 min of photocatalytic ozonation.

Among the materials prepared by the sol–gel method, only reference TiO_2 completely removed OMA when combined with ozone and radiation. On the other hand, in addition to P25, the composites with high amounts of P25 also removed all OMA. The composites were not necessarily better than the correspondent titanium dioxide during radiation containing reactions, showing that the carbon phase does not improve the performance of the semiconductor in this case. OMA, a compound highly refractory to oxidation, was completely mineralized only when ozone, radiation and some selected catalysts (TiO_2, P25, 80%P25/MWCNTs, 90%P25/MWCNTs and 80%P25/MWCNTs_oxi) were used together. The larger number of radicals produced during the photocatalytic ozonation and the consequent acceleration on the degradation process explain the results obtained.

Acknowledgments

This work was carried out with the support of Project UID/EQU/50020/2013 financed by FCT/MEC and FEDER under Programe PT2020 and research fellowship BPD/90309/2012 (Portugal).

References

[1] A. Vogelpohl, S.M. Kim, J. Ind. Eng. Chem. 10 (2004) 33–40.
[2] P.R. Gogate, A.B. Pandit, Adv. Environ. Res. 8 (2004) 501–551.
[3] V. Augugliaro, M. Litter, L. Palmisano, J. Soria, J. Photochem. Photobiol. C: Photochem. Rev. 7 (2006) 127–144.
[4] C.G. Silva, J.L. Faria, J. Mol. Catal. A: Chem. 305 (2009) 147–154.
[5] R. Rajeswari, S. Kanmani, Iran. J. Environ. Health. Sci. Eng. 6 (2009) 61–66.
[6] F.J. Beltrán, Ozone Reaction Kinetics for Water and Wastewater Systems, Lewis Publishers, Boca Raton, Florida, 2004.
[7] A. Aguinaco, F.J. Beltrán, J.F. García-Araya, A. Oropesa, Chem. Eng. J. 189–190 (2012) 275–282.
[8] T.E. Agustina, H.M. Ang, V.K. Vareek, J. Photochem. Photobiol. C: Photochem. Rev. 6 (2005) 264–273.
[9] Y. Yao, G. Li, S. Ciston, R.M. Lueptow, K.A. Gray, Environ. Sci. Technol. 42 (2008) 4952–4957.
[10] M. Mehrjouei, S. Müller, D. Möller, J. Photochem. Photobiol. A: Chem. 217 (2011) 417–424.
[11] N.K.V. Leitner, P. Berger, B. Legube, Environ. Sci. Technol. 36 (2002) 3083–3089.
[12] M. Skoumal, P.-L. Cabot, F. Centellas, C. Arias, R.M. Rodríguez, J.A. Garrido, E. Brillas, Appl. Catal. B: Environ. 66 (2006) 228–240.
[13] P.C.C. Faria, J.J.M. Órfão, M.F.R. Pereira, Appl. Catal. B: Environ. 79 (2008) 237–243.
[14] P.C.C. Faria, J.J.M. Órfão, M.F.R. Pereira, Catal. Commun. 9 (2008) 2121–2126.
[15] C.A. Orge, J.J.M. Órfão, M.F.R. Pereira, A.M. Duarte de Farias, M.A. Fraga, Chem. Eng. J. 200–202 (2012) 499–505.
[16] A.G. Gonçalves, J.L. Figueiredo, J.J.M. Órfão, M.F.R. Pereira, Carbon 48 (2010) 4369–4381.
[17] S. Garcia- Segura, E. Brillas, Water Res. 45 (2011) 2975–2984.
[18] M. Ferreira, M.F. Pinto, O.S.G.P. Soares, M.F.R. Pereira, J.J.M. Órfão, J.L. Figueiredo, I.C. Neves, A.M. Fonseca, P. Parpot, Chem. Eng. J. 228 (2013) 374–380.
[19] C.G. Silva, J.L. Faria, Photochem. Photobiol. Sci. 8 (2009) 705–711.
[20] K.S.W. Sing, D.H. Everett, R.A. Haul, W.L. Moscou, R.A. Pierotti, J. Rouquérol, T. Siemieniewska, Pure Appl. Chem. 57 (1985) 603–619.
[21] R.R.N. Marques, M.J. Sampaio, P.M. Carrapiço, C.G. Silva, S. Morales-Torres, G. Dražić, J.L. Faria, A.M.T. Silva, Catal. Today 209 (2013) 108–115.
[22] M.J. Sampaio, C.G. Silva, R.R.N. Marques, A.M.T. Silva, J.L. Faria, Catal. Today 161 (2011) 91–96.
[23] P. Kopf, E. Gilbert, S.H. Eberle, J. Photochem. Photobio. A: Chem. 136 (2000) 163–168.
[24] C. Orge, J. Sousa, F. Gonçalves, C. Freire, J. Órfão, M. Pereira, Catal. Lett. 132 (2009) 1–9.